Bull. Mater. Sci. (2021)44:77
https://doi.org/10.1007/s12034-021-02377-7

Near-white light emission from samarium and dysprosium combined doped calcium zirconate spin-coated thick film

MEENU VENUGOPAL[1], H PADMA KUMAR[2,*] and R JAYAKRISHNAN[3]
[1]Department of Physics, Mar Ivanios College, Bethany Hills, Trivandrum 695015, India
[2]Department of Physics, V.T.M.N.S.S College, Dhanuvachapuram 695503, India
[3]Department of Physics, Christian College, Chengannur 689121, India
*Author for correspondence (drhpadmakumar@gmail.com)

MS received 25 September 2020; accepted 17 November 2020

Abstract. This study investigates the preparation and characterization of $CaZr_{0.9}Sm_{0.025}Dy_{0.075}O_3$-coated film system. The powder used for coating was prepared by solid-state ceramic route synthesis and spin coating technique was used to prepare the film of the $CaZr_{0.9}Sm_{0.025}Dy_{0.075}O_3$ system. Structural studies were carried out using X-ray diffraction (XRD) and Fourier transform infrared spectroscopy. The XRD peaks of spin-coated system were indexed for an orthorhombic (Pnma) perovskite structure of $CaZrO_3$. The film when excited at 350 nm yield blue-green emission at 482 and 571 nm, which corresponds to the transition from $^4F_{9/2}$ to $^6H_{15/2}$ and $^6H_{13/2}$ levels of Dy^{3+} ion, respectively, and orange-red emission at 603 and 657 nm corresponds to the transition from $^4G_{5/2}$ to $^6H_{7/2}$ and $^6H_{11/2}$ transitions of Sm^{3+} ions, respectively. CIE coordinates of the film show near-white light emission from the system.

Keywords. Spin coating; white light emission; solid-state ceramic route; photoluminescence.

1. Introduction

Recently, inorganic perovskite films find a wide range of applications in various optoelectronic devices, display devices, photovoltaic devices and solar cells [1–4]. Various reports are available on the excellent emission properties exhibited by phosphor-coated composite films that can be used as active participants in various devices [1,2]. Various techniques, such as spin coating, spray coating, pulsed laser deposition, etc., have been used for the coating of inorganic perovskites on films [5–7]. Among various deposition techniques, spin coating has a great advantage while considering the low cost of preparation and simplicity. While considering the applications, the parameters like chemical stability and thermal stability of the perovskites used for coating is very important. On this context, zirconate perovskites had already gained widespread interest in the field of luminescent perovskites as a stable host material, as their chemical and thermal stability is very high [8–11]. They also have high melting point, which is also an important factor while considering the applications in this field [10].

Single-phase white light emitting systems are now an interesting area of research due to their improved properties over other white light emitting systems [9,12–14]. Among various zirconate perovskites, blue emission from the $[CaO_7.V''_o]$–$[CaO_7.V'_o]$ defect cluster of $CaZrO_3$ due to the oxygen vacancies makes it a promising host material for producing efficient white light emission when doped with various rare earths like samarium and dysprosium [9]. Samarium is characterized by its orange-red emission, while dysprosium by its blue-green emission [9,15,16]. Calcium zirconates is an excellent host material that can yield efficient luminescent emissions when doped with different rare earths like samarium and dysprosium [9,11,15]. Samarium- and dysprosium-doped $CaZrO_3$ systems with formula $CaZr_{0.9}Sm_xDy_{0.1-x}O_3$ have been reported as an efficient white light emitting system [9]. The addition of charge carriers like magnesium and aluminium increases the emission intensity of rare earth-doped $CaZrO_3$ systems [15]. Nevertheless, in such systems, the CIE coordinates show a shift from the value corresponding to that of white light emission. However, the nanopowders of the same systems prepared via self-propagating combustion synthesis were reported to show a huge shift in the emission properties compared to their bulk systems [11]. It is found that the emission intensity directly depend on the annealing temperature of the as-prepared samples [11]. Thus, emissions from $CaZr_{0.9}Sm_xDy_{0.1-x}O_3$ systems prepared using different methods can be tuned for different emission properties. We had reported white light emission from single-phase samarium- and dysprosium-doped $CaZrO_3$ perovskite system having formula $CaZr_{0.9}Sm_{0.025}Dy_{0.075}O_3$ with CIE coordinates (0.3310, 0.3349) prepared via solid-state ceramic route method [9].

Published online: 03 April 2021

This study discusses the preparation and emission properties of $CaZr_{0.9}Sm_{0.025}Dy_{0.075}O_3$ coated film prepared via spin coating technique.

2. Experimental

2.1 *Preparation of spin-coated film*

$CaZr_{0.9}Sm_{0.025}Dy_{0.075}O_3$ powder is first prepared by solid-state ceramic route method using high pure $CaCO_3$, ZrO_2 (Hi-media Chemicals, 99% pure) and Dy_2O_3 and Sm_2O_3 (Hi-media Chemicals, 99.9% pure) as starting materials. The starting materials were taken in stoichiometric ratios and the weighed powders were mixed thoroughly in acetone medium. This mixture was ball milled for 2 h. The prepared powder was then dried and calcined at 1225°C for about 5 h in an electrically heated furnace. The calcined powders were later grinded well. A 0.5 g of this powder sample is mixed with 5 ml of vinegar to obtain a white solution. The substrate used for the preparation of film was a well-cleaned glass film. A quantity of 250 µl of this solution was dropped on to the glass substrate and this was spun at 500 rpm for 90 s. This spin-coated substrate was then heated slowly up to 300°C in the air for 1 h [17–19]. This film with thick coating in white colour was further used for the characterization.

2.2 *Characterization methods*

The X-ray diffraction pattern of the prepared film system was studied using Philips XPERT PRO instrument using Cu-Kα radiation. Thermo-Nicolet Avatar 370 Fourier Transform Infrared (FTIR) Spectrometer was used to record the infrared (IR) spectrum of the sample and the measurement was recorded in the range 400–4000 cm^{-1}. In this study, the instrument used to record the atomic force microscopic (AFM) image was Dimension Edge, Bruker. The photoluminescence spectrum of the sample was measured using a Spectrofluorometer (Model FP 8500, Jasco International). The CIE colour coordinates based on CIE 1931 chromaticity calculations of the luminescence spectrum was also discussed.

3. Results and discussion

3.1 *XRD studies*

Figure 1 shows the X-ray diffraction (XRD) pattern of spin-coated film. All XRD peaks of figure 1 were indexed for an orthorhombic (Pnma) perovskite structure of $CaZrO_3$, which is in good agreement with the standard data (JCPDS 35-0790) [9]. The XRD pattern clearly indicates the crystalline nature of the sample. During the preparation of

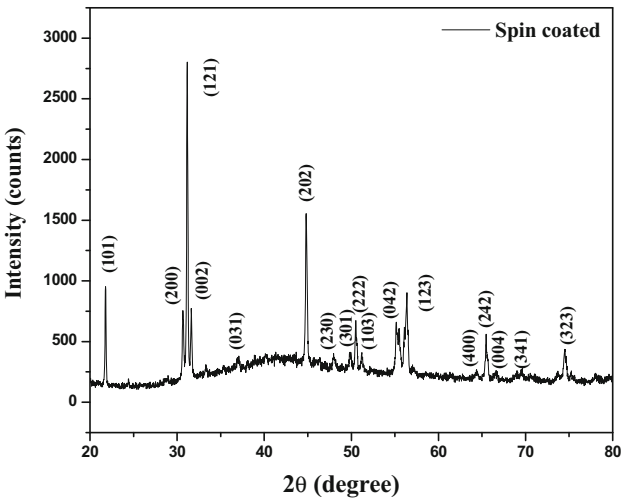

Figure 1. XRD pattern of spin-coated $CaZr_{0.9}Sm_{0.025}Dy_{0.075}O_3$ film.

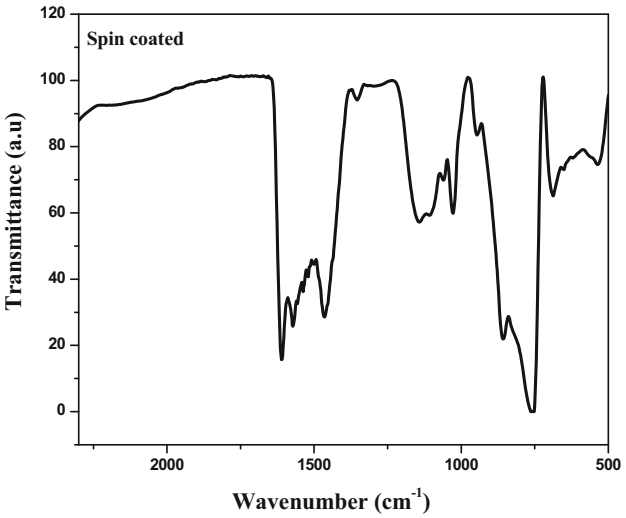

Figure 2. FTIR spectrum of spin-coated $CaZr_{0.9}Sm_{0.025}Dy_{0.075}O_3$ film.

$CaZr_{0.9}Sm_{0.025}Dy_{0.075}O_3$ powder, tetravalent Zr^{4+} ions were replaced with trivalent rare-earth ions like Sm^{3+} and Dy^{3+}. This will create a charge imbalance, which will distort the structural symmetry of the host. However due to the lower doping concentration of rare earth ions, the host structure is not highly influenced and this charge difference due to the doping will be balanced by the formation of oxygen vacancies and this will help in the efficient luminescent emissions from these systems [9,17,18].

3.2 *FTIR spectroscopy*

Figure 2 shows the FTIR spectrum of spin-coated $CaZr_{0.9}Sm_{0.025}Dy_{0.075}O_3$ system. The band at 500 cm^{-1} can be attributed to the bending vibration of Dy–O in $CaZrO_3$, while bands at 627, 756 and 872 cm^{-1} corresponds to the

stretching and bending vibrations of Zr–O in $CaZrO_3$, which is the well-known peaks of calcites [11,20–23]. The band at around 1420 cm^{-1} corresponds to the vibration of $CaZrO_3$ [11,20,24]. The bands at 1380 and 1650 cm^{-1} in figure 2 can be attributed to the bending vibrations of H–O–H water groups [18]. The band at 1033 cm^{-1} corresponds to the vibrations of samarium [11]. Broad peaks in the region of 1050–1400 in spray coated systems can be attributed to the stretching vibration and bending vibrations of –OH from Si–OH silanol groups in defect sites of glass plate used [23].

3.3 *AFM study*

Figure 3 shows the AFM analysis of spin-coated $CaZr_{0.9}Sm_{0.025}Dy_{0.075}O_3$ film. The AFM images show that there is a coagulate formation as a result of annealing of the specimen after deposition at 300°C and the grain size is in the micrometre region. This is the reason for variation in the film depth profiling as revealed from the images.

3.4 *Emission studies*

Figure 4a shows the emission spectrum of film prepared via spin coating technique. The films were excited at 350 nm. This powder system was earlier reported to yield efficient white light emission when excited at 350 nm [9]. In this study, four peaks are observed in the emission spectrum of the film when excited at 350 nm. The orange-red emission of Sm^{3+} ions arises due to the transition between $^4G_{5/2}$ to various levels, while for Dy^{3+} ion transition from $^4F_{9/2}$ to different levels give rise to blue-green emission. The spin-coated sample is showing emissions in the visible region of the electromagnetic spectrum. In figure 4, the peaks obtained at 482 and 571 nm corresponds to the transition between $^4F_{9/2} \rightarrow {}^6H_{15/2}$ and $^4F_{9/2} \rightarrow {}^6H_{13/2}$ levels of Dy^{3+} ion, respectively [9,12]. First one corresponds to the magnetic dipole transition and the second one is a hypersensitive electric dipole transition. The peak around 603 and 657 nm corresponds to the $^4G_{5/2} \rightarrow {}^6H_{7/2}$ and $^4G_{5/2} \rightarrow {}^6H_{9/2}$ transitions of Sm^{3+} ions, respectively [9]. The peak at

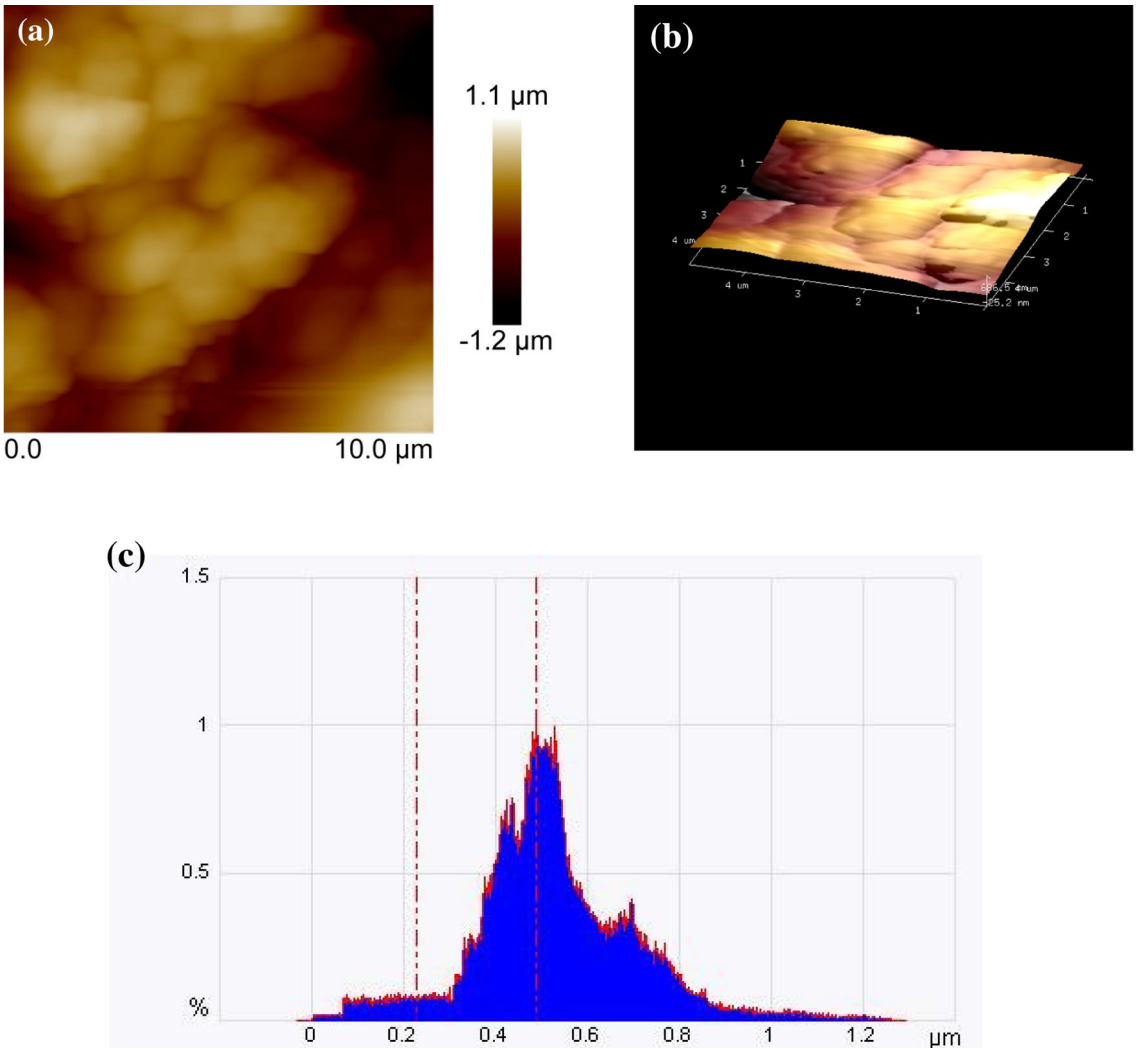

Figure 3. (**a** and **b**) AFM micrographs for the deposited film. (**c**) Depth profiling for deposited film.

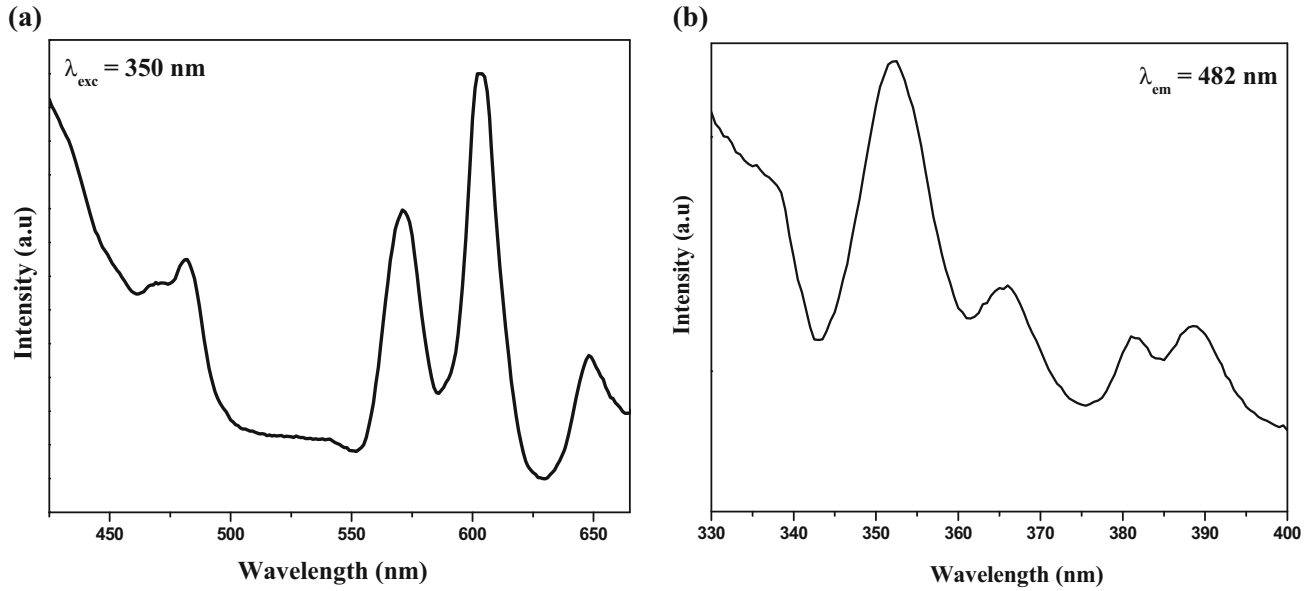

Figure 4. (**a**) Emission and (**b**) excitation spectra of spin-coated $CaZr_{0.9}Sm_{0.025}Dy_{0.075}O_3$ film.

603 nm is magnetic dipole allowed electric dipole dominated transition and one at 657 nm is a forced electric dipole transition. This electric dipole transitions highly depends on the host symmetry and they are in normal cases forbidden. Only in the cases like $CaZrO_3$ hosts having lower symmetry, these peaks will be permitted [9]. The film system shows variation in the emission intensities under an excitation of 350 nm when compared with the reported corresponding powder systems [9]. For corresponding powder samples at 354 nm excitation, the intensity of emission peaks corresponding to the $^4G_{5/2} \rightarrow {}^6H_{7/2}$ and $^4G_{5/2} \rightarrow {}^6H_{9/2}$ transitions of Sm^{3+} ions were comparatively less [9]. However, in the case of film system, at 354 nm excitation, intensity of peaks at 571 and 603 nm has increased. This change in intensity has shifted the CIE coordinates of film system to (0.3704, 0.3842) when compared with the CIE coordinates of their corresponding powder samples (0.3310, 0.3349) [9].

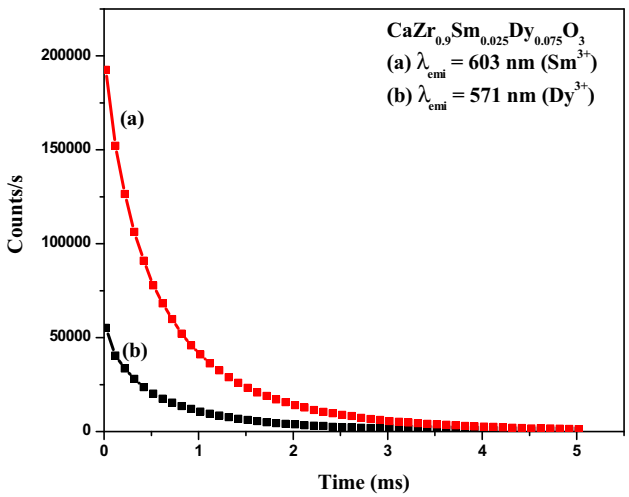

Figure 5. Decay curves of $CaZr_{0.9}Sm_{0.025}Dy_{0.075}O_3$ film.

3.5 *Excitation studies*

Figure 4b shows the excitation spectra of the spin-coated $CaZr_{0.9}Sm_{0.025}Dy_{0.075}O_3$ film monitoring emission at 482 nm. The excitation bands are centred at 350 ($^4M_{15/2}$, $^6P_{7/2}$), 365 ($^6H_{15/2}$–$^4I_{11/2}$) and 381 nm ($^6H_{15/2}$–$^4I_{13/2}$, $^4F_{7/2}$) that shows splitting corresponds to the electronic transitions of Dy^{3+} ions.

3.6 *Lifetime studies*

Figure 5 gives the decay curves corresponding to the emissions at 571 and 603 nm of the $CaZr_{0.9}Sm_{0.025}Dy_{0.075}O_3$ film excited at 350 nm. The emission at 571 nm corresponds to the transition between energy levels of Dy^{3+} ions, while the emission at 603 nm corresponds to that of Sm^{3+} ions. Lifetime τ is calculated using the equation $I = I_0 \exp(-t/\tau) + B$, where I and I_0 are the intensities, τ is the lifetime and B the background, and χ^2-values are in the range of 0.98–0.99. The experimental data of the luminescence decay was fit into a single exponential decay following the above equation, indicating that the uniform activator distribution in the crystalline host is in agreement with the XRD results given in figure 1. The lifetime of the emissions at 571 nm is found to be of the order of 0.54 ms, while for the emission at 603 nm is found to be 0.32 ms.

The chromaticity coordinates calculated from the luminescence spectrum of spin-coated $CaZr_{0.9}Sm_{0.025}Dy_{0.075}O_3$ film excited at 350 nm is given in figure 6. The CIE colour coordinates of photoluminescence spectrum of

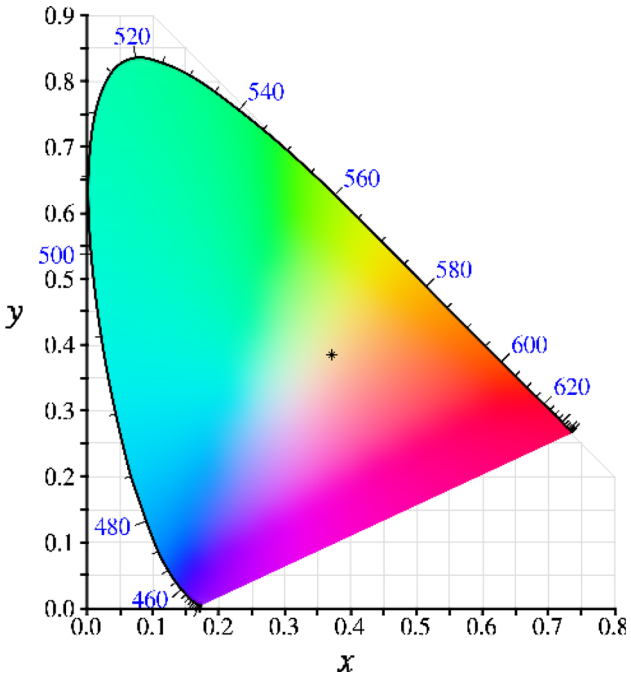

Figure 6. CIE chromaticity coordinates of spin-coated $CaZr_{0.9}Sm_{0.025}Dy_{0.075}O_3$ film.

corresponding specimen excited at 350 nm were obtained as (0.3704, 0.3842), indicating near-white light emission from the film.

4. Conclusions

Spin coating technique was used to prepare $CaZr_{0.9}Sm_{0.025}Dy_{0.075}O_3$ film and its properties were studied. The XRD pattern of the spin-coated system confirms the orthorhombic phase of $CaZrO_3$. The AFM images revealed the coagulation effect due to annealing of specimen. The emission peaks of spin-coated systems consist of peaks corresponding to the transition between various levels in samarium as well as dysprosium ions. The CIE colour coordinates of this system was calculated to be (0.3704, 0.3842). The results indicate that spin-coated rare earth-doped perovskites systems can efficiently produce emission peaks with appreciable intensity in visible range of electromagnetic spectrum. Further tuning can also yield efficient white light emitting film systems, which may find applications in various display and optoelectronic devices.

Acknowledgements

We acknowledge Sophisticated Test and Instrumentation Centre at Cochin University of Science and Technology and Kerala University Sophisticated Instrumentation and Computation Centre for providing analysis facilities.

References

[1] Braly I L, deQuilettes D W, Pazos-Outón L M, Burke S, Ziffer M E, Ginger D S *et al* 2018 *Nat. Photonics* **12** 355
[2] Zhou Q, Bai Z, Lu W G, Wang Y, Zou B and Zhong H 2016 *Adv. Mater.* **28** 9163
[3] Ball J M, Lee M M, Hey A and Snaith H J 2013 *Energy Environ. Sci.* **6** 1739
[4] Wang P, Zhang X, Zhou Y, Jiang Q, Ye Q, Chu Z *et al* 2018 *Nat. Commun.* **9** 1
[5] Liang Y, Yao Y, Zhang X, Hsu W L, Gong Y, Shin J *et al* 2016 *AIP Adv.* **6** 015001
[6] Hsu H L, Chen C P, Chang J Y, Yu Y Y and Shen Y K 2014 *Nanoscale* **6** 10281
[7] Barrows A T, Pearson A J, Kwak C K, Dunbar A D, Buckley A R and Lidzey D G 2014 *Energy Environ. Sci.* **7** 2944
[8] Kumar H P, Kumar S S, Venugopal M, Binila R, Nissamudeen K M, Thomas J K *et al* 2015 *J. Alloys Compd.* **629** 173
[9] Venugopal M, Padma Kumar H, Satheesh R and Jayakrishnan R 2019 *Int. J. Appl. Ceram. Technol.* **16** 1228
[10] Prasanth C S, Kumar H P, Pazhani R, Solomon S and Thomas J K 2008 *J. Alloys Compd.* **464** 306
[11] Venugopal M, Kumar H P, Satheesh R and Jayakrishnan R 2020 *Phys. Lett. A* **384** 126280
[12] Li G, Geng D, Shang M, Zhang Y, Peng C, Cheng Z *et al* 2011 *J. Phys. Chem. C* **115** 21882
[13] Choi S, Yun Y J and Jung H K 2012 *Mater. Lett.* **75** 186
[14] Kim J S, Jeon P E, Choi J C, Park H L, Mho S I and Kim G C 2004 *Appl. Phys. Lett.* **84** 2931
[15] Venugopal M, Kumar H P, Satheesh R and Jayakrishnan R 2019 *Mater. Res. Express* **6** 076201
[16] Venugopal M, Kumar H P and Jayakrishnan R 2020 *J. Electroceram.* **44** 163
[17] Ilican S, Caglar Y and Caglar M 2008 *J. Optoelectron. Adv. M* **10** 2578
[18] Venugopal M, Kumar S S, Nissamudeen K M and Kumar H P 2016 *J. Mater. Sci. Mater. Electron.* **27** 9496
[19] Bedyal A K, Kumar V, Sharma V, Singh F, Lochab S P, Ntwaeaborwa O M *et al* 2014 *J. Mater. Sci.* **49** 6404
[20] Evangeline B, Azeem P A, Rao R P, Swati G and Haranath D 2017 *J. Alloys Compd.* **705** 618
[21] Sommerdijk N A, van Leeuwen E N, Vos M R and Jansen J A 2007 *CrystEngComm* **9** 1209
[22] Madej D, Szczerba J and Dul K 2014 *Thermochim. Acta* **597** 27
[23] Yin W Z, Li D, Luo X M, Yao J and Sun Q Y 2016 *Int. J. Miner. Metall. Mater.* **23** 373
[24] Ballem E, Azeem A, Rayavarapu P R and Divi H 2017 *Luminescence* **32** 1246